# Cohesive communities in dynamic brain functional networks

Yongchen Fan,[1] Qiang Fan,[1] Lv Zhou,[1,2] Rong Wang,[3] Pan Lin,[4,*] and Ying Wu[1,2,†]

[1]*State Key Laboratory for Strength and Vibration of Mechanical Structures and School of Aerospace Engineering, Xi'an Jiaotong University, Xi'an 710049, China*

[2]*National Demonstration Center for Experimental Mechanics Education, Xi'an Jiaotong University, Xi'an 710049, China*

[3]*College of Science, Xi'an University of Science and Technology, Xi'an 710049, China*

[4]*Department of Psychology and Cognition and Human Behavior Key Laboratory of Hunan Province, Hunan Normal University, Changsha 410081, China*

(Received 23 December 2020; revised 17 April 2021; accepted 21 May 2021; published 2 July 2021)

In large-scale brain network dynamics, brain nodes switching between modules has been found to correlate with cognition. However, how the brain nodes engage in this kind of reorganization of modules is unclear. Based on a functional magnetic resonance imaging dataset, we construct dynamic brain functional networks and investigate nodal module temporal dynamic behavior by applying the multilayer network analysis approach. We reveal three cohesive communities that are groups of brain nodes linked in the same community during brain module dynamic reorganization. We show that the cohesive communities have higher clustering coefficients and lower characteristic path lengths than the controlled community, indicating cohesive communities are the parts of brain networks with high information processing efficiency. The smaller sample entropy of functional connectivity in cohesive communities also proves their property of being more "static" compared with the controlled community in brain dynamics. Specifically, compared with the controlled community, the functional connectivity of cohesive communities is restricted strictly by structure connectivity and shows more similarity to structure connectivity. More importantly, we find that the cohesive communities are stable not only in the resting state but also when processing cognitive tasks. Our results not only show that cohesive communities may be the fundamental community organization to support brain network dynamics but also provide insights into the intrinsic structural relationship between the resting state and task states of the brain.

DOI: 10.1103/PhysRevE.104.014302

## I. INTRODUCTION

Complex network science has been widely used to unravel the function of brain dynamics [1–3]. In the context of a complex network, neural elements such as brain regions at different scales are treated as the nodes, and their direct structural connectivity (SC) or functional interactions are regarded as the edges. Previous studies have evaluated the topological and dynamical behaviors of brain functional networks (BFNs), which are highly connected with multiple brain cognitive functions [4–7]. In addition, brain disorders, such as attention deficit hyperactivity disorder [8,9], schizophrenia [10], and Alzheimer's disease [11], are often associated with the alterations of patterns in functional connectivity (FC).

In BFN, there are groups of densely connected nodes, which are called modules or communities [12–14]. Modularity is an important character of BFN and provides a source of separation of specialized functions with various cognitive demands [15–17]. To fit different cognitive states, the FC of two distinct brain regions could be strong or weak dynamically, leading to reconfiguration of brain modules [18–20]. For example, changes of modular organization of BFN have been identified during human learning [21] and listening behavior [22]. A number of recent studies have also revealed the decrease of modularity across the human life-span [23–25]. In the module reorganization process, every node in the network can possibly switch between different modules temporally [21,26]. The high correlation between the flexibility of nodes switching across modules and the performance of higher-order cognitive tasks has been clarified [27]. However, recent studies suggest that, both in model networks and realistic networks such as social networks, there are groups of nodes that are usually found together in the same module and essentially indivisible in multiple module divisions [28]. These groups of nodes, which are called "building blocks" in Ref. [28], may represent the fundamental organization of module structures in networks. However, their functions in the networks are not fully clear. Furthermore, whether this type of community is present in brain networks has not yet been explored.

In the present work, we assume there are similar underlying "building blocks" in BFN, in which the nodes are cohesive and always join the same community during modular reorganization. We call them "cohesive communities." We first analyze module switching dynamics of nodes by applying the multilayer network analysis approach to a group of functional magnetic resonance imaging (fMRI) data acquired from 110 healthy subjects. The multilayer network analysis enables us to decompose BFN dynamics into nonoverlapping modules

*linpan@hunnu.edu.cn
†wying36@mail.xjtu.edu.cn

 

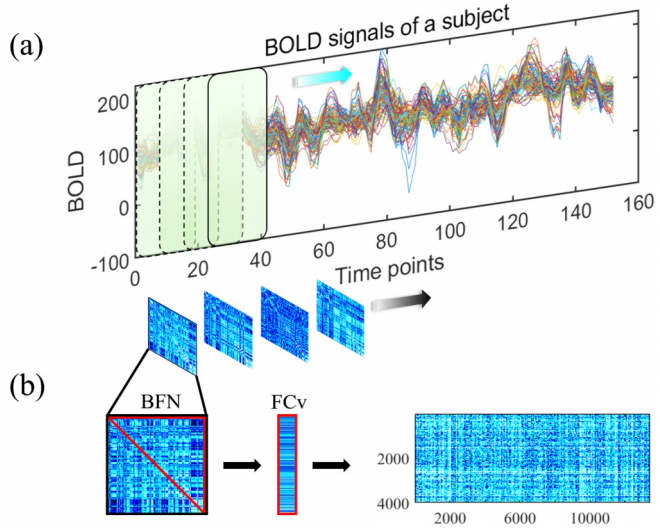


FIG. 1. The pipeline of brain dynamic FC analysis. (a) The time series are the BOLD signals of one subject after fMRI data preprocessing. Utilizing an overlapping sliding-time window approach, the dynamic BFNs were constructed. (b) The upper triangular element without a diagonal of each BFN matrix is reshaped to a column (FCv) as the matrix is symmetric. Then, all of the new columns are arranged into a new matrix in chronological order and according to the order of subjects.

that span time and space and allows us to quantify temporal switching behavior between different modules of each node [29,30]. We introduce the community solidification degree to detect the cohesive communities. The community solidification degree of one node pair is defined as the proportion of module reconfiguration events in which the node pair stays in the same module. Second, we demonstrate that the cohesive communities have higher clustering coefficients and have shorter characteristic path lengths. Furthermore, the FCs of the cohesive communities have lower sample entropy and higher similarity to SC. Finally, we verify the robustness of the cohesive communities in task states by analyzing the dynamic BFNs of four task states.

The remainder of this paper is organized as follows: Section II describes the fMRI dataset source and analysis algorithm, Sec. III describes the results of the analysis of cohesive communities, and Sec. IV gives the Discussion and Conclusions.

## II. MATERIALS AND METHODS

### A. Functional networks construction

The fMRI data used in this research were acquired from 130 healthy subjects. Twenty subjects were excluded because of incomplete data (see Supplemental Material [31]). The brain was partitioned into 90 regions of interest (ROIs) with the AAL (automated anatomical labeling) atlas [32]. The fMRI time series for each ROI was obtained by averaging the voxel time series within each ROI. An overlapping sliding-time window approach is applied to construct the dynamic BFN [Fig. 1(a)]. In this approach, a certain length time series from the first time point is cut out to construct the first BFN. The certain length time series is called a window, and its width is 30 time points. Then, the window slides forward one time point along the time series to construct the second BFN, and so on to the last time point. The set of BFNs obtained by this approach is deemed to contain brain dynamic FC information. The FC between ROIs was constructed by calculating the Pearson correlation coefficient:

$$\rho_{X,Y} = \frac{\sum_{t=1}^{N}[X(t)-\overline{X}][Y(t)-\overline{Y}]}{\sqrt{\sum_{t=1}^{N}[X(t)-\overline{X}]^2\sum_{t=1}^{N}[Y(t)-\overline{Y}]^2}}, \quad (1)$$

where $t$ is the time point, $N$ stands for the total number of time points, $X$ and $Y$ are the fMRI time series for different ROIs, and $\overline{X}$ and $\overline{Y}$ are the average values corresponding to these time series.

### B. BFN states and cohesive community detection

Processing fMRI time series of all subjects by the overlapping sliding-time window approach, the dynamic BFNs for each subject are constructed. Notably, each BFN matrix is symmetric due to ignoring directions. Therefore, the upper or lower triangular elements include FC information between all node pairs. It is reasonable that reshaping the upper triangular elements without a diagonal of every BFN matrix to a column vector (FCv) could reduce the computation and does not make the FC information incomplete; see Fig. 1(b). Then, all the FCvs are arranged into a new FCv matrix in chronological order and according to the order of subjects.

The $k$-means clustering algorithm is one of the unsupervised learning algorithms and is commonly used to cluster different observations into several clusters based on the distance between these observations [33]. It has been widely used in fMRI studies [34,35]. In the present work, the $k$-means clustering algorithm is applied to the FCv matrix to cluster all the FCvs into several clusters. Restoring the mean FCv of each cluster to the matrix can acquire the repertoire of BFN states. As it is sensitive to the initial conditions, the $k$-means clustering algorithm repeats 20 times for each $k$ from 2 to 20. The cluster result is evaluated by the maximum Dunn's score within the range of $k$ [36].

Here, we use an algorithm developed by Newman to detect the community structure of every BFN state [12]. The algorithm aimed to find the community by optimization of modularity $Q$ based on the spectral partitioning methods. The processing steps of this algorithm are as follows:

(1) Constructing a modularity matrix $B_{ij}$ for the network and finding its leading eigenvalue and eigenvector.

(2) Dividing the network into two parts according to the signs of the eigenvector elements of $B_{ij}$.

(3) Repeating steps (1) to (2) for each of the parts.

(4) Stop the processing if the split makes a zero or negative contribution to $Q$.

The $B_{ij}$ for each subgraph and $Q$ can be expressed as

$$B_{ij} = A_{ij} - \frac{k_i k_j}{2m} - \delta_{ij}\left[k_i^{(g)} - k_i\frac{d_g}{2m}\right], \quad (2)$$

$$Q = \frac{1}{2m}\left[\sum_{i,j\in g}\left(A_{ij} - \frac{k_i k_j}{2m}\right)\delta_{ij}\right], \quad (3)$$

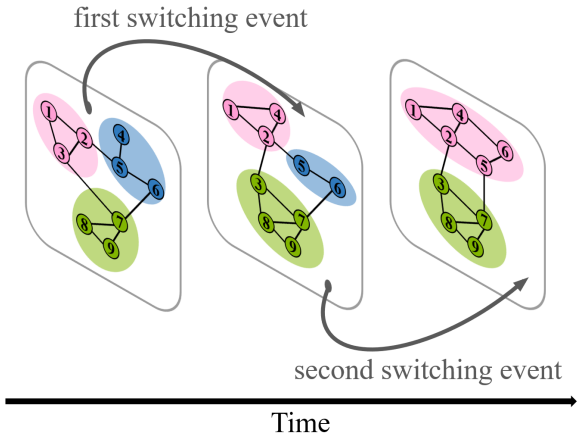


FIG. 2. A dynamic behavior example of the multilayer modular network with nine nodes and two switching events (distinct communities are shaded by different colors). The modularity partitions of the network are reorganized after each switching event. This example shows some nodes (nodes 3 and 4) joined to modules with different node groups during switching events. However, some groups of nodes (node groups {1, 2}, {5, 6}, and {7, 8, 9}) in which nodes always linked together cohesively join the same module throughout all switching events.

where $A_{ij}$ are the elements of the adjacency matrix of BFN states, $m$ is the total number of edges in the network, $k_i$ represents the degree of node $i$, $\delta_{ij} = 1$ if $i$ and $j$ are in the same community and $\delta_{ij} = 0$ otherwise, $k_i^{(g)}$ is the degree of node $i$ within subgraph $g$, and $d_g$ is the total degree of nodes in the subgraph.

To find cohesive communities, the first thing is to decide the process of brain dynamics. By applying the $k$-means clustering algorithm, the FCv matrix was reduced in dimension to several BFN states. If two adjacent FCvs relate to different BFN states, it means that the two BFN states have a switching relationship. Due to every FCv corresponding to a single BFN state, it is feasible to track the switching relationship between different BFN states. The last thing is to decide if one node pair belongs to one community both before and after a BFN state switching event; see Fig. 2 for an overview. Suppose there are $n$ BFN states with $p$ and $q$ as two states with a switching relationship along time. We define the *community solidification degree* of one node pair as the proportion of switching events in which the node pair links to the same module in all switching events between BFN states. The community solidification degree of nodes $i$ and $j$ is

$$\mathrm{SD}_{ij} = \frac{\sum_{p,q\in n} \delta_{ij,p}\delta_{ij,q}}{R}, \tag{4}$$

where $R$ is the total number of BFN state pairs that have a switching relationship, $\delta$ is the Kronecker delta function, and $\delta_{ij,p} = 1$ if $i$ and $j$ belong to the same community in state $p$. Otherwise, $\delta_{ij,p} = 0$. Observe that $\mathrm{SD}_{ij}$ is 1 if nodes $i$ and $j$ are affiliated to the same community among all of the BFN states.

### C. Analysis of cohesive communities

To illustrate the dynamic feature of cohesive communities, we analyze their node and network measures.

#### *1. Clustering coefficient*

The clustering coefficient is a typical measure of network functional segregation. It is the fraction of a node's neighbors that are also neighbors to each other [37].

$$\mathrm{CC} = \frac{1}{n}\sum_{i\in N}\frac{2t_i}{k_i(k_i-1)}, \tag{5}$$

where $n$ is the number of nodes, $N$ is the set of all nodes in the network, $t_i$ is the number of edges between the neighbors of node $i$, and $k_i$ is the degree of node $i$, which represents that node's number of neighbors.

#### *2. Characteristic path length*

The characteristic path length is the average shortest path length between all pairs of nodes in a network and is the most common measure of network functional integration [37]. The shortest path between two nodes is the least number of paths from one node to another. The path length in a weighted network usually is the inverse of connectivity strength.

$$L = \frac{1}{n}\sum_{i\in N}\frac{\sum_{i\in N, j\neq i} d_{ij}}{n-1}, \tag{6}$$

where $d_{ij}$ is the shortest path length between nodes $i$ and $j$ of the network. Note that $d_{ij} = \infty$ for all disconnected pairs $i$ and $j$.

#### *3. Sample entropy*

We used sample entropy to estimate the complexity of each dynamic FC time series between nodes in cohesive communities [38].

Using $\mathbf{X} = (x_1, x_2, \ldots, x_N)$ denote the dynamic FC time series of one node pair. Then, construct embedding vectors $V_i = (x_i, x_{i+1}, \ldots, x_{i+m-1})$, in which $m$ denotes the dimension of $V_i (1 \leqslant i \leqslant N-m+1)$. Next, calculate the Chebyshev distance between $V_i$ and other vectors. Then, define $r = \varepsilon \cdot \sigma_{\mathbf{X}}$ as a tolerance value where $\varepsilon$ is a small value fixed at 0.2 here and $\sigma_{\mathbf{X}}$ is the standard deviation of $\mathbf{X}$. The ratio between the number of vectors whose the Chebyshev distance is larger than $r$ and the total number of vectors that does not contain itself is defined as $C_i^m$:

$$C_i^m = \frac{1}{N-m}\sum_{j=1, j\neq i}^{N-m+1}\Theta(r - ||V_i - V_j||), \tag{7}$$

where $\Theta(\cdots)$ is the Heaviside function, and $||\cdots||$ stands for the Chebyshev distance.

The sample entropy of $\mathbf{X}$ is

$$S = -\ln\frac{\frac{1}{N-m}\sum_{i=1}^{N-m} C_i^{m+1}}{\frac{1}{N-m+1}\sum_{i=1}^{N-m+1} C_i^m}. \tag{8}$$

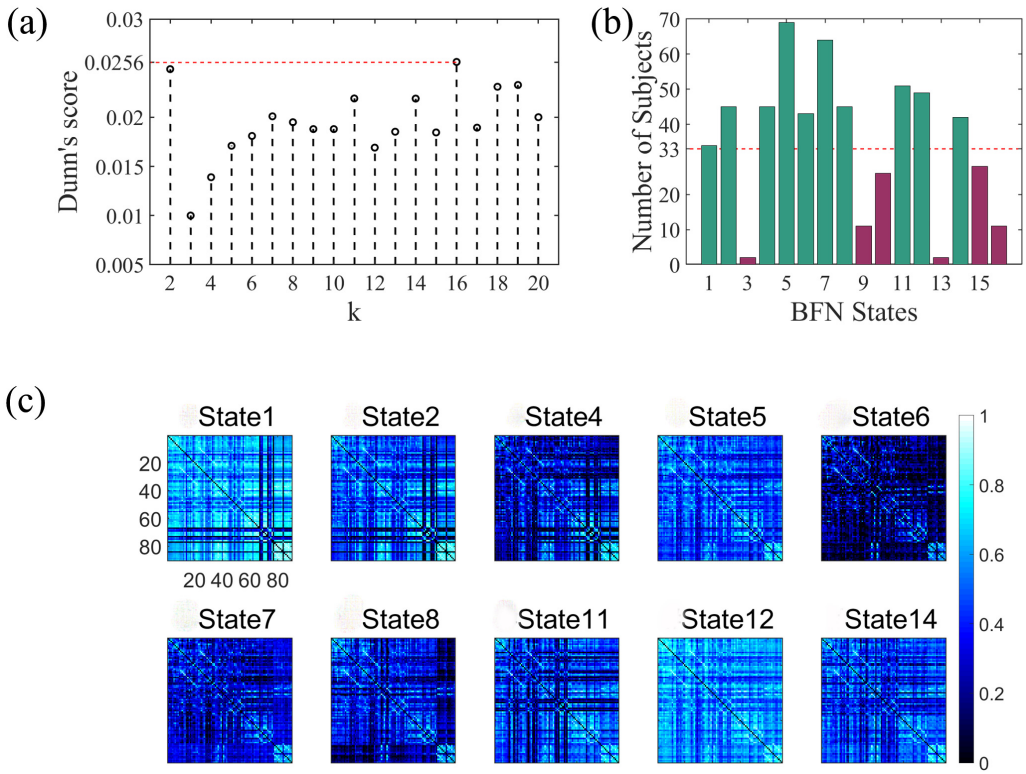


FIG. 3. (a) The Dunn's score of every $k$. The peak value of Dunn's score occurs at $k = 16$. (b) The total number of subjects who perform a certain BFN state. Of these, the BFN states that arise in more than 30% of subjects (i.e., more than 33 subjects in 110 subjects) are reserved [green (light gray) bar], and the other six BFN states are rejected [purple (dark gray) bar]. (c) The FC patterns of each BFN state.

## III. RESULTS

Based on the fMRI dataset collected from 110 healthy subjects, we first analyzed the switching dynamics of distinct BFN states by employing the multilayer network analysis approach. According to the module partition and switching relationship between different BFN states, the cohesive communities in which nodes affiliate with the same module in every BFN state are detected. We further investigate the network features of cohesive communities by calculating the clustering coefficients, characteristic path length, sample entropy, and similarity between FC and SC. Finally, we explore the robustness of the cohesive communities in task states.

### A. Cohesive communities

Using the overlapping sliding-time window approach, a total of $122 \times 110 = 13\,420$ FC windows are calculated for all subjects in the resting state. A $k$-means clustering algorithm is applied on all FCvs across time points and subjects for $k$ from 2 to 20. The results of Dunn's score in Fig. 3(a) indicate the best number of BFN states representing the present data is 16. Considering the proportion of subjects with a BFN state, we eliminate six BFN states that are only present in a few subjects [the proportion is $\leqslant$30%; see Fig. 3(b)]. The other ten BFN states that are reserved are shown in Fig. 3(c). Their FC patterns are the average of all FC window patterns identified as belonging to the BFN state by the $k$-means clustering algorithm. While every FC window corresponds to one BFN state, the FC window series can be transferred to a BFN state series across subjects. Then, the switching relationship between different BFN states can be distinguished.

The switching probabilities from one BFN state to another are shown in Fig. 4(a). The column represents the initial BFN state in a switching process, and the row is the target BFN state. For example, the value in the first row and second column means that the probability of state 1 switching to state 2 is 0.59 in all switching events from state 1. It is necessary to note that the switching behavior is considered only when the switching probability between the two BFN states $\geqslant$0.1. There are 28 potential switching events meeting the criterion. With module partition, every node (brain region) for each BFN state is assigned to a defined module. Further, whether nodes within the same module are still within one module before and after BFN state switching can be determined by the community solidification degree. The result shown in Fig. 4(b) illustrates the community solidification degrees of all node pairs, and the values that are equal to 1 (shown in orange color [dark gray)] mean the node pairs solidify to the same defined module along BFN dynamic evolution. To eliminate the effects of random factors, we apply the same analysis process to surrogate data. Finally, three cohesive communities are revealed as excluding common node pairs, for which the community solidification degrees are 1 both in real data and surrogate data. Figure 4(c) shows the community solidification degree matrix of the three cohesive communities. They are located in the anterior, middle, and posterior of the brain, respectively. The first three drawings in Fig. 4(d) display the locations of nodes in the three cohesive communities in the cortical space, respectively.

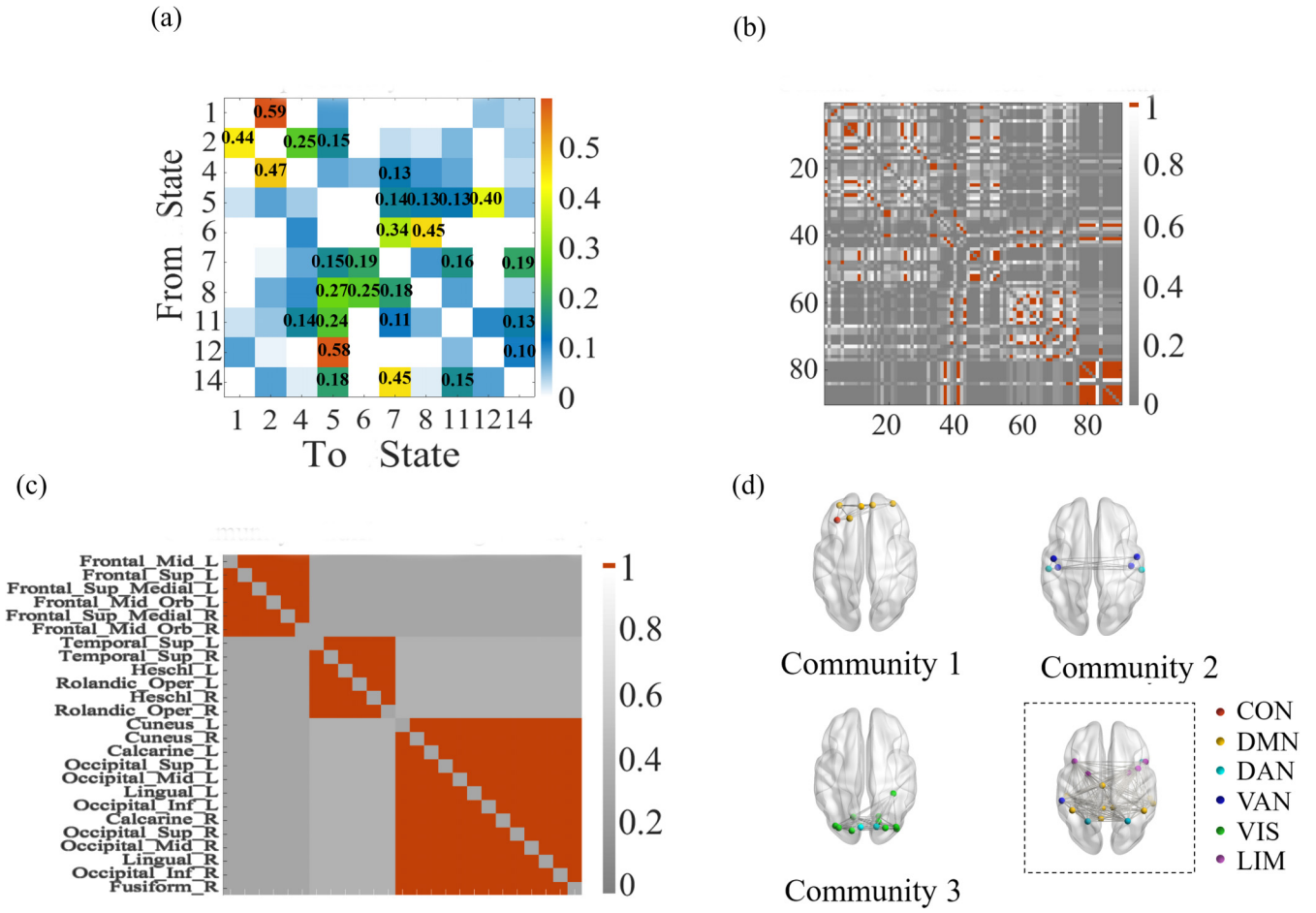


FIG. 4. (a) The probability matrix of switching between BFN states. The elements of the probability matrix mean the transition probability from one state to another. It should be noted that the elements will be considered in the present research only if the values are bigger than 0.1. (b) The community solidification degree matrix of all node pairs. The values in the matrix that are equal to 1 [shown in orange (dark gray)] meaning the node pairs solidify to the same defined module along FC dynamic evolution. (c) The community solidification degree matrix of the three cohesive communities. They include six, six, and 13 nodes, respectively. The community solidification degree equals 1 within each cohesive community. (d) The location of nodes of the three cohesive communities and the control group (in the dotted box) in cortical space.

### B. Network analysis of cohesive communities

As nodes in the three cohesive communities are special in terms of the module properties of BFNs, we wonder whether the three cohesive communities display special roles in BFN. To address this question, we first calculate the clustering coefficient and characteristic path length to clarify the functional segregation and integration of the three cohesive communities. The other 19 nodes that do not belong to the three cohesive communities are picked to constitute the control group [see the last drawing in Fig. 4(d)]. The results calculated for each BFN state show that the clustering coefficients of the three cohesive communities are higher than the control group, which means stronger functional segregation in these cohesive communities [Fig. 5(a)]. The two-sample $t$-test approach is used to confirm significant differences between cohesive communities and the control group. The results indicate the clustering coefficients of the second and the third cohesive communities are significantly higher than that of the control group. Meanwhile, the characteristic path lengths of the three cohesive communities are lower than that of the control group [Fig. 5(b)], which means stronger functional integration in these cohesive communities. The two-sample $t$-test results show the differences are significant between the control group and the second and third cohesive communities.

The cohesive communities are stable, which means they will not be broken in the dynamic switching of BFN states. This property might relate to the complexity in information processing of node pairs in cohesive communities. In other words, it is expected that FCs between node pairs in cohesive communities fluctuate so less to bond them into the same module over time. Here, sample entropy is used to estimate temporal complexity of FC between node pairs. The results show that the sample entropy of node pairs in cohesive communities is smaller than that in the control group [Fig. 5(c)]. The two-sample $t$-test results indicate the differences are significant between the control group and each cohesive community. The lower sample entropy suggests that FCs in cohesive communities are more structurally stable and less random.

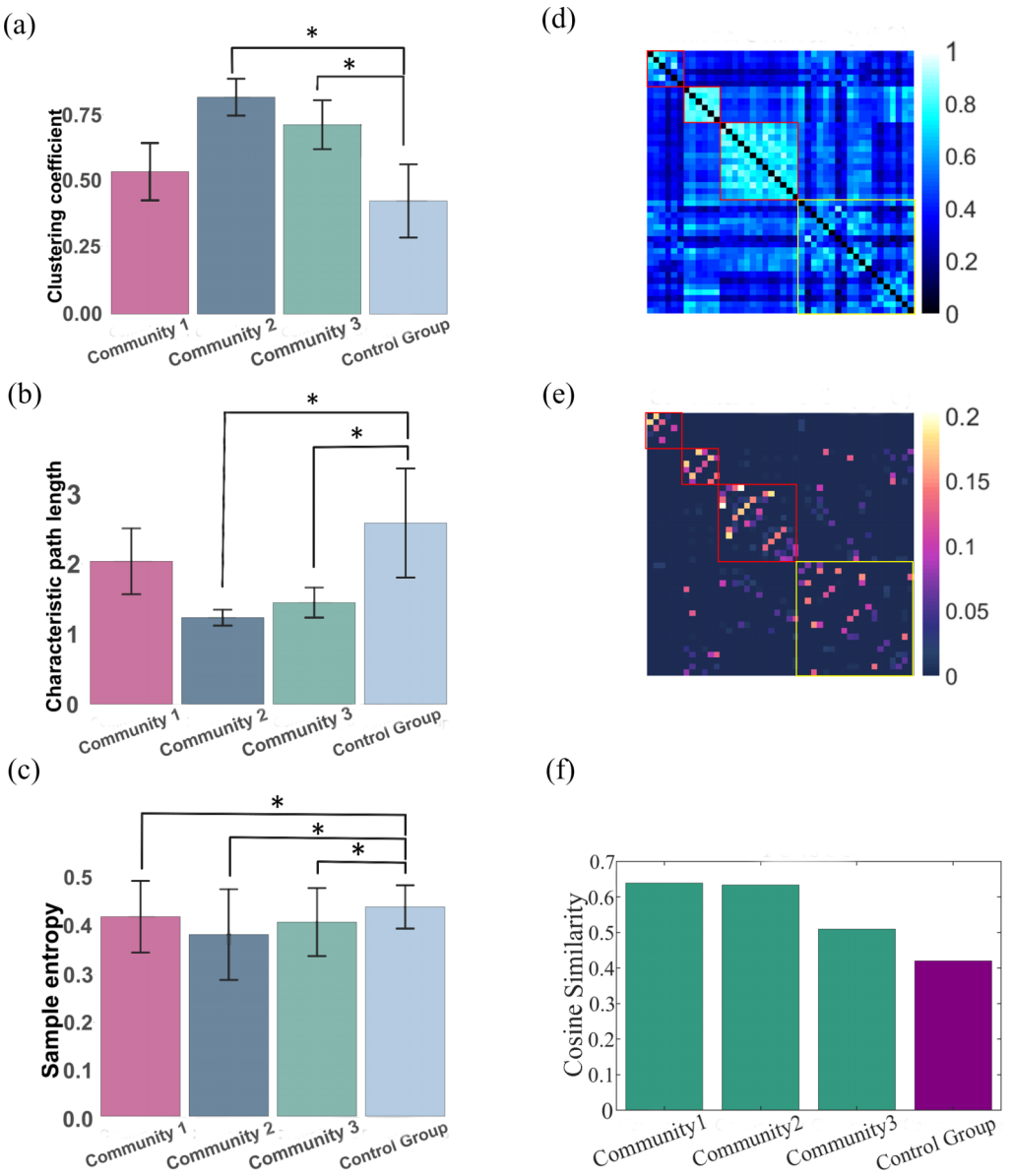


FIG. 5. (a) The clustering coefficients, (b) the characteristic path length, and (c) the sample entropy of the cohesive communities compared with the control group. The symbol "*" stands for the significant difference (two-sample $t$-test, $p < 0.05$). (d) The FC matrix of nodes in the three cohesive communities and the control group. (e) The SC matrix of nodes in the three cohesive communities and the control group. (f) The cosine similarity between values in the upper triangular parts of FC and SC within each community.

The relationship between invariant structure architecture and rich functionality of the brain has been a major mystery [39]. The following question is how the cohesive communities relate with the underlying anatomical network. The FC and SC of the three cohesive communities and the control group are shown in Figs. 5(d) and 5(e), respectively. Notably, compared with the control group [framed in yellow squares in Figs. 5(d) and 5(e)], the connectivity in both the FC and SC of cohesive communities (framed in red squares) demonstrates a significantly modular character. The results of similarity between FC and SC shown in Fig. 5(f) also indicate the FCs of cohesive communities share more features of the structure network, while the control group differs more from the structure architecture.

### C. Robustness of cohesive communities in cognitive tasks

As cohesive communities are present in resting state BFN, it is interesting to test whether the three cohesive communities will be destroyed when the brain is doing cognitive tasks. Task fMRI used here were scanned from the same subjects as resting state fMRI. These cognitive tasks include (i) the balloon analog risk task (BART), (ii) spatial working memory task (SCAP), (iii) stop-signal task, (iv) and task-switching task. For details of these tasks, see the Supplemental Material [31].

We first calculated the community solidification degree of each cognitive task BFN by applying the same research process used in resting state BFN; the results are shown in

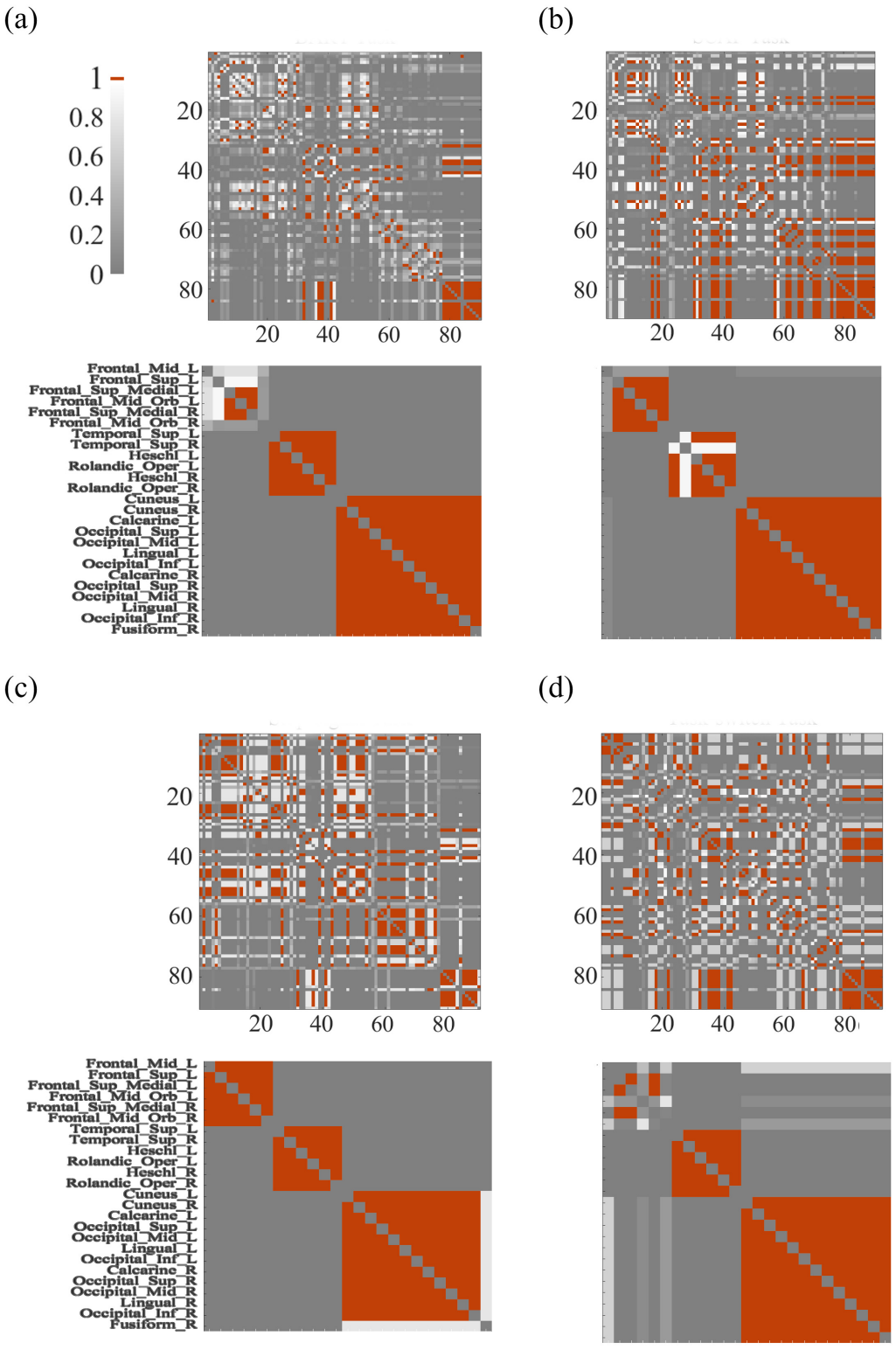


FIG. 6. The community solidification degree matrix of all node pairs (top) and the three cohesive communities (bottom) in (a) BART, (b) SCAP, (c) stop-signal task, and (d) task-switch task.

Fig. 6. The top panel of Fig. 6 shows the community solidification degree of the whole network for the four tasks. The distribution of community solidification degrees across the BFN is significantly changed by different cognitive demands. The bottom panel shows the community solidification degree matrices of the three cohesive communities. It is obvious that community solidification degrees are equal to 1 within the three cohesive communities in most cases, suggesting the brain reconfiguration under task stimulus has little influence on the modular structure of cohesive communities. Prompted

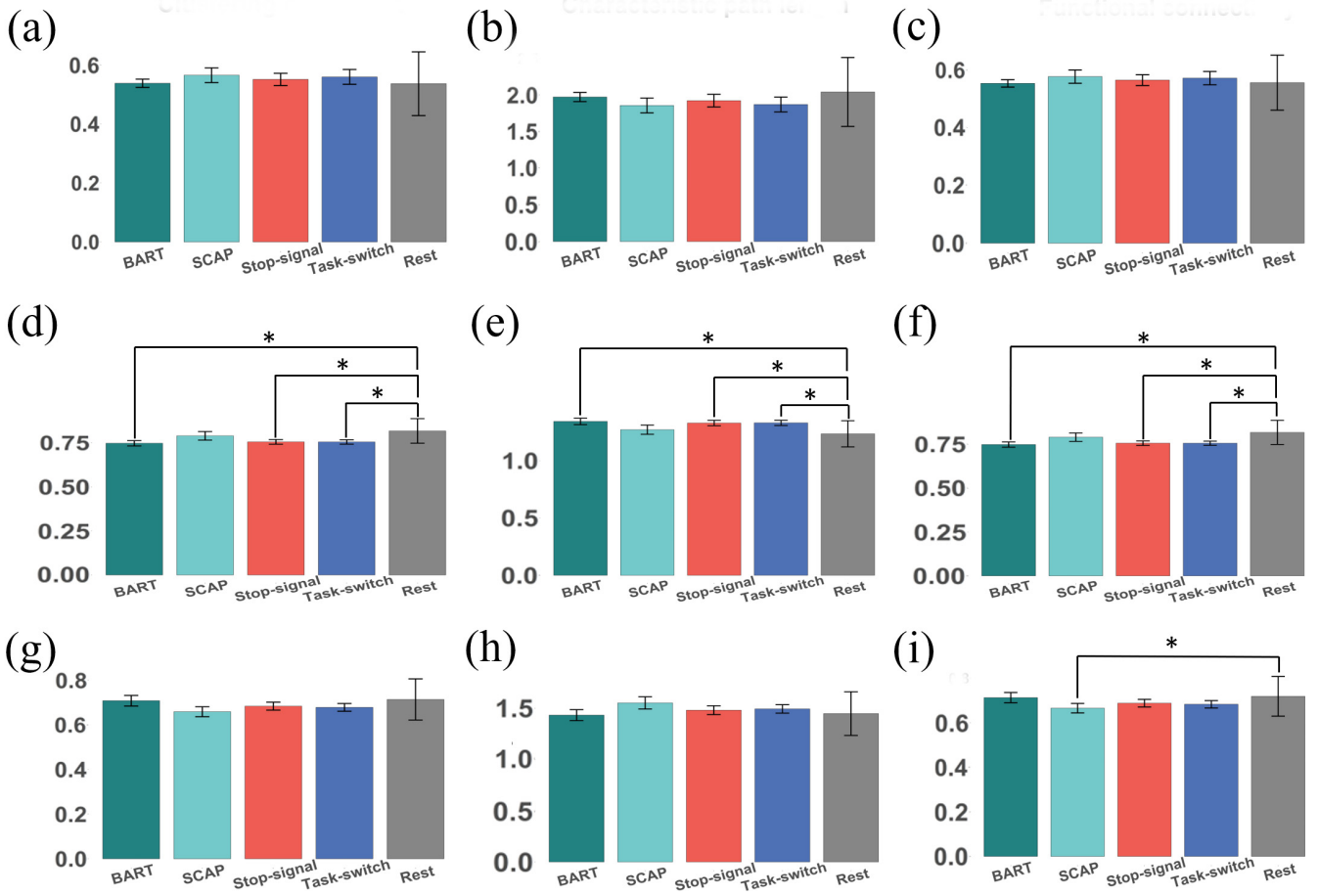


FIG. 7. The clustering coefficient (left column), characteristic path length (middle column), and FC (right column) of the three cohesive communities in all four task states (BART, SCAP, stop-signal task, and task-switch task) and resting state. The top row is for cohesive community 1, the middle row is for cohesive community 2, and the bottom row is for cohesive community 3. The symbol "*" stands for the significant difference (two-sample $t$-test, $p < 0.05$).

by these results, we wonder whether the network functional features of cohesive communities are also robust upon dynamic reconfiguration of BFN from resting state to task states. We compared the clustering coefficients, characteristic path length, and FC of the three cohesive communities in all four task states and resting state. As shown in Fig. 7, except for the FC of community 3 in the SCAP state [Fig. 7(i)], community 1 and community 3 did not perform significantly different between the task states and resting state in terms of the clustering coefficient, characteristic path length, and FC. However, the three measures of community 2 in task states are significantly different from the resting state [Figs. 7(d)–7(f)]. These results indicate that the basic modular structure of cohesive communities remains stable under task stimulus.

## IV. DISCUSSION AND CONCLUSIONS

In this paper, we investigated the nodal module temporal dynamic behavior of BFN and focused on the properties of cohesive communities. Based on the overlapping sliding-time window approach, we constructed the temporal multilayer BFN and defined the community solidification degree to detect cohesive communities. We revealed three cohesive communities in resting BFN and found that the cohesive communities had higher clustering coefficients and shorter characteristic path lengths. By investigating the complexity in information processing, we observed that the FC of cohesive communities has lower sample entropy and shows more similarity with SC. In particular, we showed that the same cohesive communities existing in the resting state are also present in task states.

The nodal switching between modules occurs in modular reconfiguration of BFN, and its relationship to brain functions has been widely explored [22,27]. However, the groups of nodes that do not exhibit module switching behavior are neglected in previous studies. A similar concept has been explored in other network science domains [28], but the functions of this kind of node have not been fully discussed. Here, we used community solidification degree to identify cohesive communities in BFNs based on multilayer network analysis. The cohesive communities comprised the nodes that did not switch between modules during brain modular reconfiguration. We found three cohesive communities located in the anterior, middle, and posterior of the brain, respectively (Fig. 4). The cohesive communities have two features. First, they are indivisible. Second, they are not independent communities but join other nodes to form larger community structures in each temporal FC. The second feature appears

to be a characteristic of hierarchical modularity. "Hierarchical module" means that a large complex network could be broken down into smaller modules that are interlinked with each other [40]. Combined with the first feature, we could speculate that cohesive communities act as the substrate layer of the hierarchical modular structure in dynamic switching between different BFN states. In BFN, the hierarchical modular structure plays an important role in supporting normal information integration and segregation processing [41]. This type of organization facilitates efficient spatial embedding, evolutionary adaptability, robustness to perturbations, and maximized functional diversity [42]. In the following discussion, we show that the cohesive communities are the more efficient parts of information processing of BFN and are robust to external task perturbations. This further demonstrates that the cohesive communities play an important functional role in supporting hierarchical modularity of BFN.

In the present work, we demonstrated the special information integration and segregation features of cohesive communities by calculating their clustering coefficients and characteristic path lengths. We found every cohesive community had higher clustering coefficients and shorter characteristic path lengths [Figs. 5(a) and 5(b)]. The clustering coefficient measures the number of triangles in the network, and a larger clustering coefficient reflects higher functional segregation [37]. Inversely, characteristic path length estimates integration of the network, with shorter path length reflecting higher integration. Simultaneously, high segregation and integration are the typical characteristics of small-world networks [43]. Furthermore, the clustering coefficients are positively correlated with local efficiency, and the characteristic path length is inversely related to global efficiency of the network [44]. Our results suggest that cohesive communities are part of BFNs with more small-worldness and higher information processing efficiency. In addition, in terms of FC-SC similarity, we found that the cohesive communities have high similarity between SC and FC. This result implies that there are more direct structural connections within functional cohesive communities. In general, a closer link to SC is found in FC during the integrated state of BFN [45]. Our findings suggest that cohesive communities may be the core to integrating BFN as densely direct SC always promotes information for global broadcast [46].

We further investigated the consistency of cohesive communities in task states, including BART, SCAP, stop-signal task, and task-switch task. Our results indicated that the three cohesive communities in the resting functional network are robust during external task perturbations. It has been demonstrated that reconfiguration of BFN across a wide variety of tasks is highly relevant to the resting state [47]. The robustness of cohesive communities in cognitive tasks confirmed the existence of the intrinsic structure in BFN during both resting state and higher-order cognitive information processing. The present results may provide potential support for the viewpoint that task-induced networks are modestly reorganized from the resting state network [5,48]. It is worth noting that "structural" stability does not mean the "functional" stability of cohesive communities in task states. We calculated clustering coefficients, characteristic path lengths, and FCs of cohesive communities in task states and showed that the second cohesive community is significantly different from the resting state. The second cohesive community consists of regions in attention networks. The high activation of attention networks in tasks may induce this kind of significant change in the second cohesive community. The correlation between cognitive performance and switching of BFN states or switching of nodes between different communities has been discussed in previous studies [4,27]. It will be important for future research to build bridges between task performance and the architecture of cohesive communities to better understand the functional role of cohesive communities in the brain.

In summary, we studied the special cohesive communities of BFN in resting state and task states. We first certified the existence of cohesive communities during brain modular reconfiguration. Second, we showed that the cohesive communities have higher clustering coefficients and shorter characteristic path lengths. Third, we found that the FCs of cohesive communities are less complex and more similar to SC. Finally, we highlighted that the same cohesive communities existing in the resting state are also present in task states. These findings not only reveal the characteristics of cohesive communities but also indicate the intrinsic relationship between the resting state and task states of the brain.

## ACKNOWLEDGMENTS

This work was supported by the National Natural Science Foundation of China (Grants No.11772242, No. 11972275, and No. 62071177), the Youth Program of the National Natural Science Foundation of China (Grant No. 12002252), and the China National Postdoctoral Fund (First Class, Grant No. 2018M631140).

[1] D. S. Bassett and O. Sporns, Network Neuroscience, Nat. Neurosci. **20**, 353 (2017).

[2] E. N. Davison, K. J. Schlesinger, D. S. Bassett, M.-E. Lynall, M. B. Miller, S. T. Grafton, and J. M. Carlson, Brain network adaptability across task states, PLoS Comput. Biol. **11**, e1004029 (2015).

[3] O. Sporns, Structure and function of complex brain networks, Dialogues Clin. Neurosci. **15**, 247 (2013).

[4] J. Cabral, D. Vidaurre, P. Marques, R. Magalhães, P. Silva Moreira, J. Miguel Soares, G. Deco, N. Sousa, and M. L. Kringelbach, Cognitive performance in healthy older adults relates to spontaneous switching between states of functional connectivity during rest, Sci. Rep. **7**, 5135 (2017).

[5] N. A. Crossley, A. Mechelli, P. E. Vértes, T. T. Winton-Brown, A. X. Patel, C. E. Ginestet, P. McGuire, and E. T. Bullmore, Cognitive relevance of the community structure of the human brain functional coactivation network, Proc. Natl. Acad. Sci. USA **110**, 11583 (2013).

[6] J. R. Cohen and M. D'Esposito, The segregation and integration of distinct brain networks and their relationship to cognition, J. Neurosci. **36**, 12083 (2016).

[7] Q. K. Telesford, M.-E. Lynall, J. Vettel, M. B. Miller, S. T. Grafton, and D. S. Bassett, Detection of functional brain network reconfiguration during task-driven cognitive states, Neuroimage **142**, 198 (2016).

[8] Y. Fan, R. Wang, P. Lin, and Y. Wu, Hierarchical integrated and segregated processing in the functional brain default mode network within attention-deficit/hyperactivity disorder, PLoS One **14**, e0222414 (2019).

[9] R. Wang, L. Wang, Y. Yang, J. Li, Y. Wu, and P. Lin, Random matrix theory for analyzing the brain functional network in attention deficit hyperactivity disorder, Phys. Rev. E **94**, 052411 (2016).

[10] J. M. Sheffield and D. M. Barch, Cognition and resting-state functional connectivity in schizophrenia, Neurosci. Biobehav. Rev. **61**, 108 (2016).

[11] S. Si, B. Wang, X. Liu, C. Yu, C. Ding, and H. Zhao, Brain network modeling based on mutual information and graph theory for predicting the connection mechanism in the progression of Alzheimer's disease, Entropy **21**, 300 (2019).

[12] M. E. J. Newman, Modularity and community structure in networks, Proc. Natl. Acad Sci. USA **103**, 8577 (2006).

[13] M. A. Bertolero, B. T. T. Yeo, and M. D'Esposito, The modular and integrative functional architecture of the human brain, Proc. Natl. Acad. Sci. USA **112**, E6798 (2015).

[14] O. Sporns and R. F. Betzel, Modular brain networks, Annu. Rev. Psychol. **67**, 613 (2016).

[15] J. Power, A. Cohen, S. Nelson, G. Wig, K. Barnes, J. Church, A. Vogel, T. Laumann, F. Miezin, B. Schlaggar, and S. Petersen, Functional network organization of the human brain, Neuron **72**, 665 (2011).

[16] R. Wang, M. Liu, X. Cheng, Y. Wu, A. Hildebrandt, and C. Zhou, Segregation, integration and balance of large-scale resting brain networks configure different cognitive abilities, Proc. Natl. Acad. Sci. USA **118**, e2022288118 (2021).

[17] R. Wang, X. Su, Z. Chang, Y. Wu, and P. Lin, Flexible brain transitions between hierarchical network segregation and integration predict human behavior (2020).

[18] J. M. Shine, O. Koyejo, and R. A. Poldrack, Temporal metastates are associated with differential patterns of time-resolved connectivity, network topology, and attention, Proc. Natl. Acad. Sci. USA **113**, 9888 (2016).

[19] K. Hilger, M. Fukushima, O. Sporns, and C. Fiebach, Temporal stability of functional brain modules associated with human intelligence, Hum. Brain Mapp. **41**, 3 (2019).

[20] A. B. A. Stevner, D. Vidaurre, J. Cabral, K. Rapuano, S. F. V. Nielsen, E. Tagliazucchi, H. Laufs, P. Vuust, G. Deco, M. W. Woolrich, E. Van Someren, and M. L. Kringelbach, Discovery of key whole-brain transitions and dynamics during human wakefulness and non-REM sleep, Nat. Commun. **10**, 1035 (2019).

[21] D. S. Bassett, N. F. Wymbs, M. A. Porter, P. J. Mucha, J. M. Carlson, and S. T. Grafton, Dynamic reconfiguration of human brain networks during learning, Proc. Natl. Acad. Sci. USA **108**, 7641 (2011).

[22] M. Alavash, S. Tune, and J. Obleser, Modular reconfiguration of an auditory control brain network supports adaptive listening behavior, Proc. Natl. Acad. Sci. USA **116**, 660 (2019).

[23] D. Meunier, S. Achard, A. Morcom, and E. Bullmore, Age-related changes in modular organization of human brain functional networks, Neuroimage **44**, 715 (2009).

[24] R. F. Betzel, L. Byrge, Y. He, J. Goñi, X.-N. Zuo, and O. Sporns, Changes in structural and functional connectivity among resting-state networks across the human lifespan, Neuroimage **102**, 345 (2014).

[25] L. Geerligs, R. J. Renken, E. Saliasi, N. M. Maurits, and M. M. Lorist, A Brain-wide study of age-related changes in functional connectivity, Cereb. Cortex **25**, 1987 (2015).

[26] Q. K. Telesford, A. Ashourvan, N. F. Wymbs, S. T. Grafton, J. M. Vettel, and D. S. Bassett, Cohesive network reconfiguration accompanies extended training, Hum. Brain Mapp. **38**, 4744 (2017).

[27] M. Pedersen, A. Zalesky, A. Omidvarnia, and G. D. Jackson, Multilayer network switching rate predicts brain performance, Proc. Natl. Acad. Sci. USA **115**, 13376 (2018).

[28] M. A. Riolo and M. E. J. Newman, Consistency of community structure in complex networks, Phys. Rev. E **101**, 052306 (2020).

[29] M. De Domenico, Multilayer modeling and analysis of human brain networks, GigaScience **6**, 1 (2017).

[30] S. F. Muldoon and D. S. Bassett, Network and multilayer network approaches to understanding human brain dynamics, Philos. Sci. **83**, 710 (2016).

[31] See Supplemental Material at http://link.aps.org/supplemental/10.1103/PhysRevE.104.014302 for more details about cognitive task and fMRI data preprocessing.

[32] N. Tzourio-Mazoyer, B. Landeau, D. Papathanassiou, F. Crivello, O. Etard, N. Delcroix, B. Mazoyer, and M. Joliot, Automated anatomical labeling of activations in SPM using a macroscopic anatomical parcellation of the MNI MRI single-subject brain, Neuroimage **15**, 273 (2002).

[33] A. K. Jain, M. N. Murty, and P. J. Flynn, Data clustering: A review, ACM Comput. Surv. **31**, 264 (1999).

[34] L. Nanetti, L. Cerliani, V. Gazzola, R. Renken, and C. Keysers, Group analyses of connectivity-based cortical parcellation using repeated *k*-means clustering, Neuroimage **47**, 1666 (2009).

[35] B.-Y. Park, K.-J. Tark, W. M. Shim, and H. Park, Functional connectivity based parcellation of early visual cortices, Hum. Brain Mapp. **39**, 1380 (2018).

[36] J. C. Dunn, A fuzzy relative of the ISODATA process and its use in detecting compact well-separated clusters, J. Cybern. **3**, 32 (1973).

[37] M. Rubinov and O. Sporns, Complex network measures of brain connectivity: Uses and interpretations, Neuroimage **52**, 1059 (2010).

[38] Y. Jia and H. Gu, Sample entropy combined with the *k*-means clustering algorithm reveals six functional networks of the brain, Entropy **21**, 1156 (2019).

[39] H.-J. Park and K. Friston, Structural and functional brain networks: From connections to cognition, Science **342**, 1238411 (2013).

[40] C. C. Hilgetag and M.-T. Hütt, Hierarchical modular brain connectivity is a stretch for criticality, Trends Cognit. Sci. **18**, 114 (2014).

[41] R. Wang, P. Lin, M. Liu, Y. Wu, T. Zhou, and C. Zhou, Hierarchical Connectome Modes and Critical State Jointly Maximize Human Brain Functional Diversity, Phys. Rev. Lett. **123**, 038301 (2019).

[42] D. Meunier, R. Lambiotte, and E. T. Bullmore, Modular and hierarchically modular organization of brain networks, Front. Neurosci. **4**, 200 (2010).

[43] D. J. Watts and S. H. Strogatz, Collective dynamics of small-world networks, Nature **393**, 440 (1998).

[44] A. Strang, O. Haynes, N. D. Cahill, and D. A. Narayan, Generalized relationships between characteristic path length, efficiency, clustering coefficients, and density, Soc. Network Anal. Min. **8**, 14 (2018).

[45] M. Fukushima, R. F. Betzel, Y. He, M. P. van den Heuvel, X.-N. Zuo, and O. Sporns, Structure-function relationships during segregated and integrated network states of human brain functional connectivity, Brain Struct. Funct. **223**, 1091 (2018).

[46] M. Shanahan, The brain's connective core and its role in animal cognition, Philos. Trans. R. Soc., B **367**, 2704 (2012).

[47] M. W. Cole, D. S. Bassett, J. D. Power, T. S. Braver, and S. E. Petersen, Intrinsic and task-evoked network architectures of the human brain, Neuron **83**, 238 (2014).

[48] L. J. Hearne, L. Cocchi, A. Zalesky, and J. B. Mattingley, Reconfiguration of brain network architectures between resting-state and complexity-dependent cognitive reasoning, J. Neurosci. **37**, 8399 (2017).